

COMPUTATIONAL PHYSICS - PROJECT 4

DAHL, JON KRISTIAN
 FLØISAND, JOHAN ANDREAS
 SAND, MATS OLA

Draft version November 19, 2019

ABSTRACT

For most systems in statistical mechanics it is practically impossible to analytically compute thermodynamic properties due to the amount of particles and the dependence on the partition function. We therefore turn to computers to find approximate expressions for properties like the internal energy, or the magnetic susceptibility of a system. This report studies how we can find thermodynamic properties of a system modelled by the Ising model. Some of the tools we use to solve the system include Monte Carlo simulations of Markov chains (MCMC) together with the Metropolis algorithm. We find that our calculations yield very good result against the analytical expressions for a 2×2 lattice, with errors as low as $\epsilon_{\langle E \rangle} \approx 6.67 \cdot 10^{-5} E/J$ for 10^9 Monte Carlo cycles (MCc). We find that the equilibrium time is greater for larger temperatures, with $4 \cdot 10^5$ MCcs for $\tilde{T} = 2.4k_B T/J$ and $5 \cdot 10^3$ MCcs for $\tilde{T} = 1k_B T/J$. The calculations reveal that the energy distribution of the systems, which are scaled by the total number of spins in the lattice, have a standard deviation of $\sigma_{2.4} \approx 0.14283E/J$ for $\tilde{T} = 2.4k_B T/J$ and $\sigma_1 \approx 0.00766E/J$ for $\tilde{T} = 1k_B T/J$. Finally, we find that the calculated critical temperature of the 100×100 lattice approximates the critical temperature of the infinite spin lattice with a value of $\tilde{T}_C(L \rightarrow \infty) \approx 2.27517k_B T/J$. The error of this calculation is $\epsilon_{T_C(L \rightarrow \infty)} \approx 0.00598k_B T/J$ from the analytical value of $T_C(L \rightarrow \infty) \approx 2.269k_B T/J$ given by [Onsager \(1944\)](#).

1. INTRODUCTION

To describe what we observe in nature, we create mathematical models which aim to fit empirical data. The description of macroscopic effects due to certain microscopic configurations can be particularly hard to model due to the vast amount of microscopic particles, and the astronomical number of possible configurations such a system may harbor. Magnetism in a material is a macroscopic manifestation of certain microscopic configurations. When a sufficient amount of electrons in a material point in the same direction, the material becomes magnetic. A successful model of magnetic systems is the Ising model. In this report we study how different thermodynamic properties can be found numerically for a system governed by the Ising model. We do this by a Monte Carlo method on a Markov chain, applying the Metropolis algorithm. We also see how good our numerical results corresponds with the analytical results from [Onsager \(1944\)](#).

We begin our report with a theory section where we give a brief explanation of the Ising model, as well as the Monte Carlo method we will be using. An explanation of Markov chains and the Metropolis algorithm follows. We then continue with a method section explaining how we chose to implement the Metropolis algorithm and how we have derived the different thermodynamic variables of interest. Next, a combined result and discussion section give the numerical result as well as the error. We here also compare our result with that of [Onsager \(1944\)](#). Finally we have a conclusion where we explain our main results and give our thoughts for improvement and further analysis.

An appendix is also included due to long and relatively uninteresting in-between calculations, as well as various

figures which are better suited with having their own three last pages.

All code used to generate data for this report is available at the GitHub repository <https://github.com/johanaf1/FYS3150-4150/tree/master/project4>.

2. THEORY

2.1. Ising model

The Ising model on a square lattice studies a system with the Hamiltonian

$$\mathcal{H} = -J \sum_{\langle ij \rangle} s_i s_j, \quad (1)$$

where $s_i = \pm 1$ for convenience is called the spin at site i , J is the exchange interaction (which in this case favours parallel alignment) and the index $\langle ij \rangle$ tells us to sum over the nearest neighbours ([Yeomans 1992](#), chapter 1.2). This system has already been solved by [Onsager \(1944\)](#) and we will use the analytical value for the critical temperature to evaluate our results later.

It is common to add a Zeeman term for the energy in a magnetic field ([Plischke & Bergersen 1994](#), chapter 3.1)

$$\mathcal{H} = -J \sum_{\langle ij \rangle} s_i s_j - H \sum_i s_i,$$

but in this report we let $H = 0$.

Our Hamiltonian (1) involves a magnetic term and the partition function $Z(T, H)$ therefore depends on the magnetic field strength H . Important features of our system are the internal energy $\langle E \rangle$ and magnetization $\langle M \rangle$. From these we are able to find ([Yeomans 1992](#), chapter

2.2-2.7) the heat capacity at constant volume,

$$C_V = \left(\frac{d\langle E \rangle}{dT} \right)_V = \frac{\sigma_E}{k_B T^2}, \quad (2)$$

and the susceptibility at constant temperature,

$$\chi_T = \left(\frac{d\langle M \rangle}{dH} \right)_T = \frac{\sigma_M}{k_B T}. \quad (3)$$

When solving this system numerically to find the values of interest, $\langle E \rangle$, $\langle M \rangle$, C_V and χ , we do not know the values of J and s_i . We therefore choose to normalize our variables:

$$\tilde{E} = E/J \quad \tilde{T} = k_B T/J \quad \tilde{M} = M/a$$

This gives us

$$\sigma_E^2 = \langle E^2 \rangle - \langle E \rangle^2 = \langle (\tilde{E}J)^2 \rangle - \langle \tilde{E}J \rangle^2 = J^2 (\langle \tilde{E}^2 \rangle - \langle \tilde{E} \rangle^2) = J^2 \sigma_{\tilde{E}}^2.$$

Hence, we can calculate

$$C_V = \frac{\sigma_E^2}{k_B T^2} = \frac{J^2 \sigma_{\tilde{E}}^2}{k_B (\tilde{T}J/k_B)^2} = k_B \frac{\sigma_{\tilde{E}}^2}{\tilde{T}^2}.$$

In the same manner

$$\sigma_M^2 = \langle M^2 \rangle - \langle M \rangle^2 = \langle (\tilde{M}a)^2 \rangle - \langle \tilde{M}a \rangle^2 = a^2 (\langle \tilde{M}^2 \rangle - \langle \tilde{M} \rangle^2) = a^2 \sigma_{\tilde{M}}^2$$

and thus

$$\chi_T = \frac{\sigma_M^2}{k_B T} = \frac{a^2 \sigma_{\tilde{M}}^2}{k_B (\tilde{T}J/k_B)} = \frac{a^2}{J} \frac{\sigma_{\tilde{M}}^2}{\tilde{T}}.$$

Through out this report we will be more interested in the value

$$\chi = \frac{a^2}{J} \frac{\sigma_{\tilde{M}}^2}{\tilde{T}}.$$

2.2. Monte Carlo simulations

For small lattices, such as a 2×2 lattice, we are able to compute the partition function by hand and thus also the variables of interest. For larger lattices this becomes very difficult without the results from [Onsager \(1944\)](#). We therefore turn to Monte Carlo algorithms to solve the system.

The basic philosophy behind Monte Carlo algorithms are to draw finitely many random numbers from the probability distribution of our system to enable us to compute values of interest. For many systems, such as multidimensional integrals, Monte Carlo algorithm proves to be very efficient. For the Ising model we want to map the unknown probability distribution of the system, without computing it directly. We do this with the help of a Markov chain and the Metropolis-Hastings algorithm.

2.3. Markov chains

Since we in a way are very much in the dark of what the probability distribution actually is, we will construct a Markov chain to map out the distribution. (A more rigorous approach to Markov chains are given in [Robert](#)

& [Casella 1999](#), chapter 6), and lighter introduction is given in ([Landau & Binder 2000](#), chapter 2).)

Following the approach given in ([Plischke & Bergersen 1994](#), chapter 7), suppose that the system is in a given microstate i . The next state j in the sequence is selected with a transition probability $P_{j \leftarrow i}$ that does not depend on the previous history of the system. Under fairly general conditions such a process produces states with a *unique* steady-state probability distribution.

For the Ising model, we wish to determine a transition matrix $P_{i \leftarrow j}$ so that the steady-state distribution is

$$\pi(i) = \frac{e^{-\beta E_i}}{Z} \quad (4)$$

where Z is the partition function. We generating a sequence of states from an initial state i by choosing a site α randomly and attempt to *flip* (change the sign of) its spin. The resulting state (which may be the same state i if the attempt to flip σ_α fails) we call j . Let $P_{j \leftarrow i}$ be the transition probability $i \rightarrow j$. After n steps the transition probability $P_{f \leftarrow i}(n)$ is given by

$$P_{f \leftarrow i}(n) = \sum_{i_1, i_2, \dots, i_{n-1}} P_{f \leftarrow i_{n-1}} P_{i_{n-1} \leftarrow i_{n-2}} \dots P_{i_1 \leftarrow i}$$

After many steps the system will approach a limiting distribution

$$\pi(f) = \lim_{n \rightarrow \infty} P_{f \rightarrow i}(n)$$

independently of the initial configuration. We achieve the desired distribution (4) by requiring the probability distribution to be normalized and to satisfy

$$\frac{\pi(m)}{\pi(j)} = e^{-\beta(E(m) - E(j))}$$

for all pairs of states m, j . We now also require the transition probabilities to be normalized

$$\sum_j P_{j \leftarrow m} = 1 \quad (5)$$

and to obey

$$\frac{P_{j \leftarrow m}}{P_{m \leftarrow j}} = \frac{\pi(j)}{\pi(m)} = e^{-\beta(E(j) - E(m))}. \quad (6)$$

We find that

$$\pi(m) = \sum_j P_{j \leftarrow m} \pi(m) = \sum_j P_{m \leftarrow j} \pi(j). \quad (7)$$

The first step in (7) follows from normalization (5) while the second step involves substituting (6). Equation (6) is called the *principle of detailed balance* and we see that it is a sufficient condition for arriving at the correct limiting probability distribution, provided that our process for selecting moves does not contain any “traps”, i.e. it should always be possible to get from any given microstate to any other microstate.

2.4. Metropolis algorithm

To achieve detailed balance we use the Metropolis algorithm ([Plischke & Bergersen 1994](#), chapter 7):

- (i) Pick a site α randomly.

- (ii) Compute the energy change $\Delta E = E(j) - E(i)$ that would occur if the spin at site α were flipped.
- (iii) If $\Delta E \leq 0$, flip the spin at site α ; if $\Delta E \geq 0$ flip this spin with probability $e^{-\beta\Delta E}$.
- (iv) Repeat steps (i) to (iii) until enough data is collected.

Step (iii) can be thought of as blindly accepting spin configurations that give lower energy, and accepting spin configurations that give higher energy with a given probability. It can be shown that this algorithm fulfills our requirements for convergence to the actual distribution (Robert & Casella 1999, chapter 6).

3. METHOD

3.1. Initializing the $n \times n$ lattice

The configuration of the spin lattice will initially be in one of two categories of states: An ordered state where all the spins are of equal value, or a random state where all the spins are of a random value. This definition is ambiguous for sufficiently small lattice sizes since randomly drawn spin values may yield a spin lattice with all spins +1 or all spins -1. For a 2×2 lattice the probability for an all spin +1 or -1 configuration drawn randomly where all spins are of equal probability, is 1 in 16 since each spin can be one of two values and there are 2×2 spins. At a lattice of only 4×4 the probability of this happening is so low that this will never happen at the calculation scale we are performing, with a probability of 1 in 65,536. We generate a random initial spin lattice for every temperature we are performing the calculation on, and the number of temperatures is on the scale 20 to 40, which are far from 65,536.

With a lattice size of 20×20 we are guaranteed to start at a highly disordered randomly drawn initial state, far from the ordered all +1 or all -1 state, which enables us to study the convergence behaviour of the initially ordered and initially random spin lattices. In practice, the calculation of the initial random state is done by drawing either +1 or -1 using the PRNG Mersenne Twister 19937. The ordered initial state is simply calculated by setting all the spins to +1.

3.2. Monte Carlo cycles and metropolis algorithm

When the lattice is initialized, we calculate the initial total energy and magnetization of the system for a chosen temperature T . For this given temperature, we perform $n \times n$ flips of randomly drawn spins in the lattice, which we define as one Monte Carlo cycle (MCc).

Flipping the spins can be done in two ways: One way is to perform all the $n \times n$ flips consecutively, and then fetching the total energy for the system. If the new total energy is lower than the old total energy, we accept it; if not, we do a Metropolis check on the newly calculated energy difference. The Metropolis check is done by drawing a random number, $r \in [0, 1)$, and checking if $r \leq e^{-\Delta E}$, where ΔE is the difference in energy for the lattice from the old to the new configuration. If this is fulfilled, the spin flip will be accepted.

Another way to perform the MCc is to check the energy difference for a given spin flip every time we flip a random

spin. For this method we calculate the energy difference should the spin be flipped, perform the Metropolis check on the energy difference, and finally carry out the spin flip if the Metropolis algorithm tells us to do so. For a spin in the lattice with four surrounding spins, we know that its energy can be $E \in \{-4J, -2J, 0, 2J, 4J\}$. When a flip is done, the new energy will always be $-2 \times$ the energy the given grid point had before the flip. We use this knowledge to pre-calculate the allowed values of the energy difference so that we can fetch the values from memory instead of calculating them every time. As with the first way of performing the MCc we always execute the flip if $\Delta E < 0$, and if not, we do the Metropolis check for accepting or declining the flip.

Of the two ways of performing the MCc described here, we have chosen the second edition.

3.3. Convergence and temperature dependence for the lattice

In the process of finding the convergence point of the system, we store the total energy and the total magnetic moment for the system after each MCc. The convergence time will be determined by studying a plot of the calculated values of $\langle E \rangle$ and $\langle |M| \rangle$ as a function of MCcs. When $\langle E \rangle$ and $\langle |M| \rangle$ have settled down sufficiently, we say that the system has converged to the most likely values of $\langle E \rangle$ and $\langle |M| \rangle$. We use the absolute value of the mean magnetic moment instead of the mean magnetic moment itself. This is because the absolute value behaves in a much more orderly fashion than the raw value itself, and the absolute value will therefore converge much faster. Even though the two values are not the same, we can still use the absolute value to draw relevant conclusions in this study as we will see in later sections.

When we study the temperature dependence of different lattice sizes, we are only interested in the values when the systems have become stable. The process is to run the stable systems for a given amount of MCcs while calculating the averages $\langle E \rangle$, $\langle E^2 \rangle$, $\langle M \rangle$, $\langle M^2 \rangle$, and $\langle |M| \rangle$ on the fly. Since there is only need for storing the final average values and not the total energy and total magnetic moment for every MCc, the datasets will be much smaller. The data before convergence will simply be discarded based on the convergence time described in the previous paragraph, and they will not be included in the averaged values. When all the data has been calculated, the total energy, absolute value of the total magnetic moment, heat capacity at constant volume and magnetic susceptibility will be plotted as a function of temperature to visualize the temperature dependence. This part of the study includes lattices of sizes 20×20 , 40×40 , 60×60 , 80×80 and 100×100 .

Note that since we use the absolute value of the magnetic moment instead of the magnetic moment itself, the magnetic susceptibility will not be the proper magnetic susceptibility, since it is properly calculated with M and not $|M|$.

3.4. Analysing the probability distribution

The probability distribution is determined by how many times each total energy value occurs during the calculation, which we visualize using a histogram. When the system has converged, we will see a distribution of the

total energy situated around the most probable energy value. The histogram will reveal the shape of the distribution and from the histogram data we will make a normalised probability distribution function. We study the standard deviation of the probability distribution function for both ordered initial and random initial systems to determine whether the initial state affects the distribution of the energy values. We will also study the histogram to determine the connection between the system temperature and the most probable total energy.

3.5. Phase transitions and critical temperatures

What will ultimately come out of the averages $\langle E \rangle$, $\langle E^2 \rangle$, $\langle M \rangle$, $\langle M^2 \rangle$, and $\langle |M| \rangle$ for all the different lattice sizes when the systems have converged, is the peculiar phenomenon of a phase transition. At a certain temperature the lattice of spins will experience a maximum heat capacity and a maximum magnetic susceptibility. This temperature is called a critical temperature, and is dependent on the size of the lattice.

Because of the limited capabilities of computers, in accordance with memory and processing power, we are restricted to study lattices of very small sizes compared to real life materials. The largest lattice we study is of 100×100 spins. A hand sized chunk of magnetic material is astronomically huge compared to this, with more than $6 \cdot 10^{23}$ spins. We therefore want to use the calculated critical temperatures for all lattice sizes to approximate the critical temperature for a lattice where the number of spins $\rightarrow \infty$. The exact critical temperature for a system of spins $\rightarrow \infty$ is given by (Onsager (1944))

$$\frac{k_B T_C}{J} = \frac{2}{\ln(1 + \sqrt{2})} \approx 2.269. \quad (8)$$

By using the expression (Hjorth-Jensen (2019))

$$T_C(L) - T_C(L \rightarrow \infty) = aL^{-1/\nu}, \quad (9)$$

we can solve for $T_C(L \rightarrow \infty)$, plug in the calculated critical temperature for a given lattice size and check this number against the exact value in eq. (8). To do this, we first need to determine the constant, a .

To determine the constant a , we first solve equation (9) with respect to a . Then we use the analytical expression for the time derivative of the heat capacity of the 2×2 lattice, as described in equation (A1) in the appendix, to find the maximum value of the heat capacity. We then extract the accompanying temperature value which is the critical temperature for the 2×2 lattice. By this method, we get an estimate on the constant a and a possibility to use the maximum heat capacity data of the different spin lattices to estimate the critical temperature for a lattice of infinite size.

3.6. 2×2 lattice

Looking at a 2×2 lattice we have 6 possible states, with (d) degeneration levels (the subscripts in the first state are indices for later use):

1. ($d = 1$)

\uparrow_4	\uparrow_3
\uparrow_1	\uparrow_2
2. ($d = 4$)

\uparrow	\uparrow	\uparrow	\uparrow	\downarrow	\downarrow	\uparrow
\downarrow	\uparrow	\uparrow	\downarrow	\uparrow	\uparrow	\uparrow
3. ($d = 4$)

\uparrow	\uparrow	\uparrow	\downarrow	\downarrow	\downarrow	\uparrow
\downarrow	\downarrow	\uparrow	\downarrow	\uparrow	\uparrow	\downarrow
4. ($d = 2$)

\uparrow	\downarrow	\downarrow	\uparrow
\downarrow	\uparrow	\uparrow	\downarrow
5. ($d = 4$)

\downarrow	\downarrow	\downarrow	\downarrow	\uparrow	\uparrow	\downarrow
\uparrow	\downarrow	\downarrow	\uparrow	\downarrow	\downarrow	\downarrow
6. ($d = 1$)

\downarrow	\downarrow
\downarrow	\downarrow

The energy for a state is given by the equation

$$E = -J \sum_{\langle kj \rangle} s_k s_l, \quad (10)$$

where k indicates a spin, and l indicates the neighbouring spins of k . $\langle kj \rangle$ means that we sum the four neighbouring spins of k . When calculating the energy for all the spins, we use periodic boundary conditions. Periodic boundary conditions means that the neighbours to the right of the spins in the rightmost column are the spins in the leftmost (the first) column. Equivalently for all the edge cases. The lattice behaves as if it is wrapped around to make all the ends meet. For an example, we'll use the above setting, let's say for spin 1 in configuration 2:

$$\begin{array}{ccc} & \uparrow_4 & \uparrow_3 \\ \uparrow_2 & \downarrow_1 & \uparrow_2 \\ & \uparrow_4 & \end{array}$$

Notice that spin 2 and spin 4 appears two times, since they are both the real neighbours to spin 1, and the wrapped around neighbours of spin 1. A spin appearing twice is only the case for a 2×2 lattice, where the neighbour to the right can also be the neighbour to the left, due to the periodic boundary conditions. Any greater lattice size will not let this happen.

The magnetic moment is given by

$$M = \sum_i s_i = s_{\uparrow} - s_{\downarrow}, \quad (11)$$

where s_{\uparrow} is the number spins up, and s_{\downarrow} is the number spins down. An other interesting value is the absolute value of the magnetic moment

$$|M| = \sum_i s_i = |s_{\uparrow} - s_{\downarrow}|. \quad (12)$$

	Analytical	Numerical	Error
$\langle M \rangle, [M/a]$	3.99464293	3.99461358	$2.935099 \cdot 10^{-5}$
$\langle E \rangle, [E/J]$	-7.98392834	-7.98386162	$6.671975 \cdot 10^{-5}$
$C_v, [k_B]$	0.12832933	0.12885987	$5.305454 \cdot 10^{-4}$
$\chi, [a^2/J]$	0.01604296	0.01615196	$1.090044 \cdot 10^{-4}$

TABLE 1

COMPARISON OF THE NUMERICAL AND ANALYTICAL RESULTS FOR THE SIMPLE 2x2 LATTICE USING 10^9 MONTE CARLO ITERATIONS AND $\tilde{T} = 1$ THE TEMPERATURE IS IN UNITS OF $k_B K/J$ WHERE k_B IS THE BOLTZMANN CONSTANT AND J IS THE INTERACTION STRENGTH BETWEEN NEIGHBOURING SPINS.

With the partition function as

$$Z = \sum_i e^{-\beta E_i}.$$

we can calculate the following values for the 2×2 lattice, with all the calculation steps included appendix A:

The expectation value of the energy:

$$\langle E \rangle = -8J \frac{\sinh(8J\beta)}{3 + \cosh(8J\beta)}.$$

The mean absolute value of the magnetic momentum:

$$\langle |M| \rangle = 2 \frac{2 + e^{8J\beta}}{3 + \cosh(8J\beta)}.$$

The expectation value of the squared energy:

$$\langle E^2 \rangle = (8J)^2 \frac{\cosh(8J\beta)}{3 + \cosh(8J\beta)}.$$

The heat capacity:

$$C_V = \frac{(8J)^2 \beta}{T} \frac{3 \cosh(8J\beta) + 1}{(3 + \cosh(8J\beta))^2}.$$

The expectation value of the square of the magnetic moment:

$$\langle |M|^2 \rangle = \langle M^2 \rangle = 8 \frac{1 + e^{8J\beta}}{3 + \cosh(8J\beta)}.$$

The magnetic susceptibility:

$$\chi_{|M|} = 4\beta \frac{3 + 2e^{8J\beta} + 2 \cosh(8J\beta)}{(3 + \cosh(8J\beta))^2}$$

4. RESULTS AND DISCUSSION

4.1. 2x2 lattice

Table 1 shows the numerical and analytical results of the 2x2 lattice. The numerical calculation was done with 10^9 Monte Carlo iterations and yielded a good agreement with errors of $\propto 10^{-4}$ and $\propto 10^{-5}$. What amounts to a "good agreement" is dependent on what kind of calculations the numbers may be used for, and we have set the good agreement to be errors in the 10^{-4} region and less.

Table 2 shows the analytical values for the energy, absolute value of the magnetic moment and the corresponding degree of degeneration for all the six possible configurations of a 2×2 lattice.

Number of \uparrow	Degeneration	E	$ M $
4	1	-8J	4
3	4	0	2
2	4	0	0
2	2	8J	0
1	4	0	2
0	1	-8J	4

TABLE 2

THE ENERGY, ABSOLUTE VALUE OF THE MAGNETIC MOMENT, AND THE CORRESPONDING DEGENERATION DEGREE FOR EACH OF THE SIX POSSIBLE CONFIGURATIONS OF THE 2×2 LATTICE.

4.2. When will the most likely state be reached?

Figures 1 and 2 show the convergence times for $\tilde{T} = 1k_B T/J$ and $\tilde{T} = 2.4k_B T/J$ respectively. The convergence times are represented as the number of Monte Carlo cycles (MCcs), where one MCc is one sweep of the spin lattice. 10 individual runs were made for initial ordered and initial random states at both temperatures. The cumulative average data from each run is displayed as grey graphs and the average of all the grey graphs are displayed as the black graphs. By averaging over a set of data, we get a more accurate representation of the expected behaviours of the systems. The spread of the grey graphs represent the variances between the different runs, and the black graphs represents the expectation values of the different configurations.

Looking at $\tilde{T} = 1k_B T/J$, it is apparent that the random and ordered initial states yield different behaviours, but $\langle E \rangle$ converges to the same value for both the initially ordered and random state, and the same for $\langle |M| \rangle$. This is expected behaviour, since the most probable energy and magnetization is only dependent on the energy difference from one configuration to another and not the starting configuration of the lattice. The road to convergence is not the same for the two initial states, where we observe a smoother, but a much slower transition for the random initial state than for the ordered initial state. At this scale, the ordered states converges quickly after only about five thousand Monte Carlo cycles, while the random states never reaches the same level of convergence, even at 10^6 cycles. For studies of systems at this temperature, it seems that the initial ordered state is the best basis.

For $\tilde{T} = 2.4k_B T/J$ in figure 2 the y axis interval is 0.1 function values as compared to 0.006 function values in figure 1, which highlights the fact that the convergence time is longer for $\tilde{T} = 2.4k_B T/J$ than for $\tilde{T} = 1k_B T/J$. The difference between the ordered initial states and the random initial states is not as apparent for $\tilde{T} = 2.4k_B T/J$. For most practical purposes the convergence time is equal for the two configurations, and choosing $4 \cdot 10^5$ MCcs seems to be a safe starting point. What is worth noting is that the variance is greater for $\langle |M| \rangle$ than for $\langle E \rangle$. We better therefore choose the convergence point from where the variance in $\langle |M| \rangle$ seems adequately small. The variance is displayed by the spread of the cumulative average data from all the runs, which is displayed as the grey graphs.

Deciding on the convergence time is often practiced in a bit of a hand-waving way, by simply plotting the values of interest as a function of MCcs and deciding on a point of satisfying convergence by looking at the plot.

One can always adjust the axis limits to make the data look far from converged, so a proper point of convergence will depend on how the data will be used. Picking the convergence point by eye is a good starting point, but we better have in mind that convergence is a relative term in this setting.

Figure 3 shows the number of times a spin flip has been accepted, the number of accepted configurations, as a function of temperature. The data analysis has been performed in the same manner here, where each individual run is represented as the grey graphs and the black graph is the average of every individual run. The number of accepted configurations is pretty much identical for every run and for both initial starting configurations. A section has been zoomed and highlighted in both figures to accentuate the tiny differences. The number of accepted configurations increase exponentially in the given temperature interval, and the initial state hardly makes any difference in the number of accepted configurations.

4.3. Analysing the probability distribution

Figure 4 shows a histogram and a probability distribution of the total energy of the spin lattice for every Monte Carlo cycle, for temperatures $\tilde{T} = 1k_B T/J$ and $\tilde{T} = 2.4k_B T/J$. The plots show data from after the point of convergence. These points, as discussed in section 4.2, are at $5 \cdot 10^3$ and $4 \cdot 10^5$ MCs for $\tilde{T} = 1k_B T/J$ and $\tilde{T} = 2.4k_B T/J$ respectively. For temperature $\tilde{T} = 1k_B T/J$, the distribution is not much to look at. We expect to find the system in a low energy state at a low temperature, and that is what we see from both the histogram and the probability distribution. For temperature $\tilde{T} = 2.4k_B T/J$ we clearly see a distribution around the expectation value of the energy at $\tilde{E} \approx -1.24E/J$. This is in agreement with the energy convergence value for both the ordered initial state and the random initial state in figure 2.

The difference in probability distribution between the ordered initial state and the random initial state is too small to see visually. This is expected behaviour since we discard the data from before the system has converged. After convergence, the initial state of the system should not matter since the only calculational difference between the two settings is the initial configuration of the spin lattice. We can still see tiny differences in the data of the standard deviation between the initial ordered state and the initial random state. These numbers are displayed in table 3.

	Ordered	Random
$\sigma_1, [E/J]$	0.00766	0.00764
$\sigma_{2.4}, [E/J]$	0.14283	0.14295

TABLE 3

THE STANDARD DEVIATIONS OF THE ENERGY DISTRIBUTION AFTER CONVERGENCE FOR $\tilde{T} = 1k_B T/J$ AND $\tilde{T} = 2.4k_B T/J$ FOR BOTH ORDERED INITIAL AND RANDOM INITIAL STATES. THE ENERGY IS IN UNITS OF $[\tilde{E}] = E/J$ AND IS SCALED BY $\tilde{E}/(\text{NUMBER OF SPINS})$.

Since the spins in the lattice are randomly flipped, the standard deviation will never be exactly the same for two individual runs regardless if the initial states are identical or different. The differences we see in table 3 are expected statistical differences, and whether we use data

from the initially ordered or the initially random system does not matter. The initial state of the system affects only the convergence time, and it is therefore preferable to choose an initial state with short convergence time so that we don't have to discard large amounts of data. As seen in figure 1 the convergence time is shorter for the ordered state, and we will therefore gain more usable data by using an initial ordered state. If several more individual calculations are run, and they all show approximately the same standard deviation as in table 3, we may use the central limit theorem to estimate how many MCs are needed to get the standard deviation below a given threshold. Should we use these numbers for further calculations, we may want to set a restriction on how large the standard deviation can be, and we would need to adjust the number of MCs accordingly.

4.4. Numerical studies of phase transitions

Figure 5 shows $\langle \tilde{E} \rangle$, $\langle |\tilde{M}| \rangle$, \tilde{C}_V , $\tilde{\chi}_{|\tilde{M}|}$ plotted as a function of temperature for each lattice size. A critical point is clearly seen for all lattice sizes in the plots of \tilde{C}_V and $\tilde{\chi}$. The heat capacity and susceptibility both have a sharp spike at approximately the same temperature. This critical point indicates a phase transition. The plot of the heat capacity has the calculated data points plotted as dots, and interpolated graphs plotted as solid lines. The interpolation is used for finding the location of the maximum heat capacity value, and hence the corresponding critical temperature value. Table 4 shows approximations to the critical temperature a lattice with size approaching infinity, using the critical temperature data from each lattice size we have studied, and using the relation $T_c(L \rightarrow \infty) = T_c(L) - aL^{(-1/\nu)}$ Onsager (1944). Table 4 shows in the right column the difference between the analytical answer of $T_c(L \rightarrow \infty) \approx 2.269$ and the calculated value $\tilde{T}_c(L \rightarrow \infty)$. It is clear that the approximation becomes better as the lattice size gets larger.

Lattice	Calculated $\tilde{T}_c(L \rightarrow \infty), [k_B T/J]$	Error, $[k_B T/J]$
2x2	2.4	0.13081
20x20	2.30659	0.03741
40x40	2.28921	0.02002
60x60	2.28217	0.01298
80x80	2.27835	0.00916
100x100	2.27517	0.00598

TABLE 4

THE CALCULATED DATA ARE THE APPROXIMATIONS TO THE CRITICAL TEMPERATURE $T_c(L \rightarrow \infty)$ USING THE MAXIMUM HEAT CAPACITY VALUE FROM THE INTERPOLATED DATA SETS FOR ALL LATTICE SIZES. CORRESPONDING LATTICE SIZES ARE IN THE LEFT COLUMN, AND THE DIFFERENCES FROM THE KNOWN ANALYTICAL VALUE ARE DISPLAYED IN THE RIGHT COLUMN. THE ANALYTICAL VALUE IS $T_c(L \rightarrow \infty) = 2/\ln(1 + \sqrt{2}) \approx 2.269$ Onsager (1944).

5. CONCLUSION

By studying the 2×2 lattice, we have found that 10^9 Monte Carlo cycles produce numerical errors as low as $\epsilon_{\langle E \rangle} \approx 6.67 \cdot 10^{-5} E/J$, and not larger than $\epsilon_\chi \approx 1.09 \cdot 10^{-4}, [a^2/J]$. These values can also be seen in table 1.

We have seen that the equilibrium time, measured in Monte Carlo cycles, is shorter for the $\tilde{T} = 1k_B T/J$ system than for the $\tilde{T} = 1k_B T/J$ with equilibrium times of $5 \cdot 10^3$ and $4 \cdot 10^5$ Monte Carlo cycles respectively. This behaviour is seen in figures 1 and 2. The total number of accepted configurations increases exponentially in the interval $\tilde{T} \in [1, 2.25]k_B T/J$, and the number is practically identical for any initial state.

By counting the number of occurrences for each total system energy, we reveal a distribution of energies around $\tilde{E}/(20 \times 20) \approx -2.0E/J$ for $\tilde{T} = 1k_B T/J$ and a distribution of energies around $\tilde{E}/(20 \times 20) \approx -1.24E/J$ for $\tilde{T} = 2.4k_B T/J$. This can be seen in figure 4. We find that the standard deviation of the energy distribution for $\tilde{T} = 1k_B T/J$ is $\sigma_1 \approx 0.00766E/J$ and $\sigma_1 \approx 0.00764E/J$ for the ordered and the random initial states respectively.

For $\tilde{T} = 2.4k_B T/J$ we get standard deviations of $\sigma_{2.4} \approx 0.14283E/J$ and $\sigma_{2.4} \approx 0.14295E/J$ for the ordered and random initial states respectively. The data seems to reveal that any individual calculation yields approximately the same standard deviation, and the initial state of the system is irrelevant as long as we discard any value before the system has converged.

We find that the numerically calculated critical temperature for the 100×100 lattice produce an approximation to the critical temperature for an infinite lattice of $\tilde{T}_C(L \rightarrow \infty) \approx 2.27517k_B T/J$ which has an error of $0.00598k_B T/J$ from the exact known value of $T_C(L \rightarrow \infty) \approx 2.269k_B T/J$ Onsager (1944). The data for all lattice sizes can be seen in table 4.

All code used to generate data for this report is available at the GitHub repository <https://github.com/johanafl/FYS3150-4150/tree/master/project4>.

REFERENCES

- Hjorth-Jensen, M. 2019, ComputationalPhysics, <https://github.com/CompPhysics/ComputationalPhysics/blob/master/doc/Projects/2019/Project4/pdf/Project4.pdf>, GitHub
- Landau, D., & Binder, K. 2000, A Guide to Monte Carlo Simulations in Statistical Physics (Cambridge University Press)
- Onsager, L. 1944, Phys. Rev., 65, 117, doi: [10.1103/PhysRev.65.117](https://doi.org/10.1103/PhysRev.65.117)
- Plischke, M., & Bergersen, B. 1994, Equilibrium Statistical Physics (World Scientific). <https://books.google.no/books?id=eqy22vA0SfwC>
- Robert, C. P., & Casella, G. 1999, Monte Carlo Statistical Methods, Springer texts in statistics (Springer). <https://books.google.no/books?id=nlqVQgAACAAJ>
- Yeomans, J. 1992, Statistical Mechanics of Phase Transitions (Clarendon Press). <https://books.google.no/books?id=3IUVSvOUtTMC>

APPENDIX

APPENDIX: 2X2 LATTICE CALCULATIONS

With the configurations given in 3.6, we can easily calculate the total energies of the system according to (10):

$$\begin{aligned} E_1 &= -J(1 \cdot (1 + 1 + 1 + 1) + 1 \cdot (1 + 1) + 1 \cdot (1 + 1) + 1 \cdot 0) = -8J, \\ E_2 &= -J(-1 \cdot (1 + 1 + 1 + 1) + 1 \cdot (1 + 1) + 1 \cdot (1 + 1) + 1 \cdot 0) = 0, \\ E_3 &= -J(-1 \cdot (-1 - 1 + 1 + 1) - 1 \cdot (1 + 1) + 1 \cdot (1 + 1) + 1 \cdot 0) = 0, \\ E_4 &= -J(-1 \cdot (1 + 1 + 1 + 1) + 1 \cdot (-1 - 1) - 1 \cdot (1 + 1) + 1 \cdot 0) = 8J, \\ E_5 &= -J(1 \cdot (-1 - 1 - 1 - 1) - 1 \cdot (-1 - 1) - 1 \cdot (-1 - 1) - 1 \cdot 0) = 0, \\ E_6 &= -J(-1 \cdot (-1 - 1 - 1 - 1) - 1 \cdot (-1 - 1) - 1 \cdot (-1 - 1) - 1 \cdot 0) = -8J. \end{aligned}$$

The values of the magnetic moment is equally easily computed, given equation (11):

$$\begin{aligned} M_1 &= 4 - 0 = 4, \\ M_2 &= 3 - 1 = 2, \\ M_3 &= 2 - 2 = 0, \\ M_4 &= 2 - 2 = 0, \\ M_5 &= 1 - 3 = -2, \\ M_6 &= 0 - 4 = -4. \end{aligned}$$

The partition function is given by (Yeomans 1992, chapter 2)

$$Z = \sum_i e^{-\beta E_i}.$$

Setting in numbers, we find

$$Z = e^{8J\beta} + 4e^0 + 4e^0 + 2e^{-8J\beta} + 4e^0 + e^{-8J\beta} = 2e^{8J\beta} + 2e^{-8J\beta} + 12 = 12 + 4 \cosh(8J\beta),$$

and thus

$$Z = 12 + 4 \cosh(8J\beta).$$

With the energy, magnetic moment and the partition function, we can calculate the analytical expressions for the expected energy $\langle E \rangle$, expected magnetic moment $\langle M \rangle$, expected absolute magnetic moment $\langle |M| \rangle$, expected magnetic

moment squared $\langle M^2 \rangle$ and expected energy squared $\langle E^2 \rangle$. From these we can calculate the the heat capacity at constant volume C_V , and the magnetic susceptibility (at constant temperature) χ of our system, given by equation (2) and (3) respectively.

The expectation value for the energy is given by

$$\langle E \rangle = \frac{\sum_i E_i e^{-\beta E_i}}{Z} = \frac{-8J e^{8J\beta} + 2 \cdot 8J e^{-8J\beta} - 8J e^{8J\beta}}{Z} = 16J \frac{e^{-8J\beta} - e^{8J\beta}}{12 + 4 \cosh(8J\beta)} = -16J \frac{2 \sinh(8J\beta)}{4(3 + \cosh(8J\beta))},$$

and thus

$$\langle E \rangle = -8J \frac{\sinh(8J\beta)}{3 + \cosh(8J\beta)}.$$

The mean absolute value of the magnetic momentum is given by

$$\langle |M| \rangle = \frac{\sum_i |M_i| e^{-\beta E_i}}{Z} = \frac{4e^{8J\beta} + 4 \cdot 2e^0 + 4 \cdot 2e^0 + 4e^{8J\beta}}{4(3 + \cosh(8J\beta))} = \frac{16 + 8e^{8J\beta}}{4(3 + \cosh(8J\beta))} = 2 \frac{2 + e^{8J\beta}}{3 + \cosh(8J\beta)},$$

that is

$$\langle |M| \rangle = 2 \frac{2 + e^{8J\beta}}{3 + \cosh(8J\beta)},$$

The expectation value for the squared energy is given by

$$\langle E^2 \rangle = \frac{\sum_i E_i^2 e^{-\beta E_i}}{Z} = \frac{(-8J)^2 e^{8J\beta} + 2 \cdot (8J)^2 e^{-8J\beta} + (-8J)^2 e^{8J\beta}}{Z} = \frac{4 \cdot (8J)^2 \cosh(8J\beta)}{4(3 + \cosh(8J\beta))} = (8J)^2 \frac{\cosh(8J\beta)}{3 + \cosh(8J\beta)},$$

that is

$$\langle E^2 \rangle = (8J)^2 \frac{\cosh(8J\beta)}{3 + \cosh(8J\beta)}.$$

Heat capacity, given by equation (2), is

$$\begin{aligned} C_V &= \frac{\sigma_E}{k_B T^2} = \frac{\langle E^2 \rangle - \langle E \rangle^2}{k_B T^2} = \frac{(8J)^2 \frac{\cosh(8J\beta)}{3 + \cosh(8J\beta)} - (8J)^2 \left(\frac{\sinh(8J\beta)}{3 + \cosh(8J\beta)} \right)^2}{k_B T^2} \\ &= \frac{(8J)^2}{k_B T^2} \frac{3 \cosh(8J\beta) + \cosh^2(8J\beta) - \sinh^2(8J\beta)}{(3 + \cosh(8J\beta))^2} = \frac{(8J)^2}{k_B T^2} \frac{3 \cosh(8J\beta) + 1}{(3 + \cosh(8J\beta))^2} \end{aligned}$$

such that

$$C_V = \frac{(8J)^2 \beta}{T} \frac{3 \cosh(8J\beta) + 1}{(3 + \cosh(8J\beta))^2}.$$

The expectation value of the squared magnetic momentum is given by

$$\langle M^2 \rangle = \frac{\sum_i M_i^2 e^{-\beta E_i}}{Z} = 32 \frac{1 + e^{8J\beta}}{4(3 + \cosh(8J\beta))} = 8 \frac{1 + e^{8J\beta}}{3 + \cosh(8J\beta)}.$$

Susceptibility, given by equation (3), is

$$\begin{aligned} \chi_{|M|} &= \frac{\sigma_{|M|}}{k_B T} = \frac{\langle |M|^2 \rangle - \langle |M| \rangle^2}{k_B T} = \frac{8 \frac{1 + e^{8J\beta}}{3 + \cosh(8J\beta)} - 4 \left(\frac{2 + e^{8J\beta}}{3 + \cosh(8J\beta)} \right)^2}{k_B T} = 4 \frac{2(1 + e^{8J\beta})(3 + \cosh(8J\beta)) - (2 + e^{8J\beta})^2}{(3 + \cosh(8J\beta))^2 k_B T} \\ &= 4 \frac{2(3 + 3e^{8J\beta} + \cosh(8J\beta) + e^{8J\beta} \cosh(8J\beta)) - 4 + 4e^{8J\beta} + e^{16J\beta}}{(3 + \cosh(8J\beta))^2 k_B T} \\ &= 4 \frac{7(1 + e^{8J\beta}) + e^{-8J\beta} + e^{16J\beta} - 4 + 4e^{8J\beta} + e^{16J\beta}}{(3 + \cosh(8J\beta))^2 k_B T} = 4 \frac{3 + 2e^{8J\beta} + 2 \cosh(8J\beta)}{(3 + \cosh(8J\beta))^2 k_B T}, \end{aligned}$$

where we have used

$$\begin{aligned} 2(1 + e^{8J\beta})(3 + \cosh(8J\beta)) &= 2(3 + 3e^{8J\beta} + \cosh(8J\beta) + e^{8J\beta} \cosh(8J\beta)) \\ &= 6 + e^{8J\beta} + e^{-8J\beta} + e^{8J\beta} + e^{16J\beta} + 1 \\ &= 7(1 + e^{8J\beta}) + e^{-8J\beta} + e^{16J\beta}, \end{aligned}$$

and

$$2(1 + e^{8J\beta})(3 + \cosh(8J\beta)) - 4 - 4e^{8J\beta} - e^{16J\beta} = 3(1 + e^{8J\beta}) + e^{-8J\beta} = 3 + 2e^{8J\beta} + 2\cosh(8J\beta).$$

The susceptibility can thus be written as

$$\chi_{|M|} = 4\beta \frac{3 + 2e^{8J\beta} + 2\cosh(8J\beta)}{(3 + \cosh(8J\beta))^2}.$$

The time derivative of the heat capacity is given by:

$$\frac{dC_V}{dT} = \frac{2(8J)^3 \sinh\left(\frac{8J}{k_B T}\right) \left(3 \cosh\left(\frac{8J}{k_B T}\right) + 1\right)}{k_B^2 T^4 \left(\cosh\left(\frac{8J}{k_B T}\right) + 3\right)^3} - \frac{3(8J)^3 \sinh\left(\frac{8J}{k_B T}\right)}{k_B^2 T^4 \left(\cosh\left(\frac{8J}{k_B T}\right) + 3\right)^2} - \frac{2(8J)^2 \left(3 \cosh\left(\frac{8J}{k_B T}\right) + 1\right)}{k_B T^3 \left(\cosh\left(\frac{8J}{k_B T}\right) + 3\right)^2} \quad (\text{A1})$$

APPENDIX: FIGURES

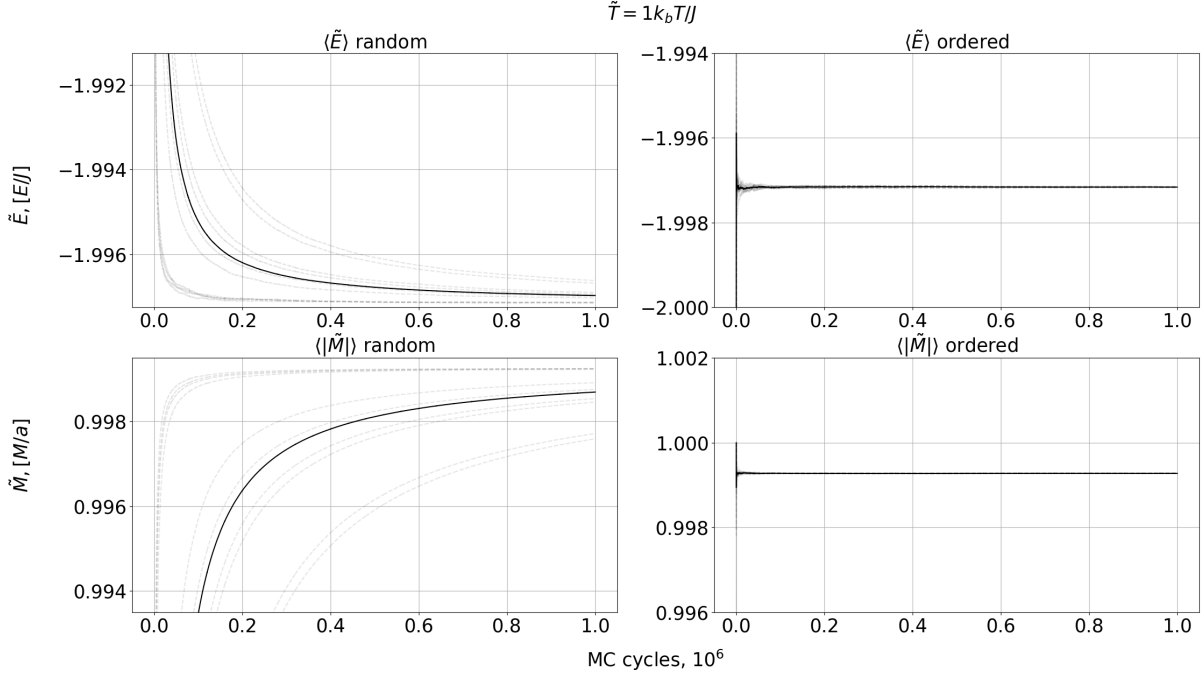


FIG. 1.— $\langle \tilde{E} \rangle$ and $\langle \tilde{M} \rangle$ as a function of Monte Carlo cycles at $\tilde{T} = 1k_B T/J$ for ordered and random initial states. The y values are scaled with $1/(\text{total spins})$, and the plotted y intervals are of 0.006 function values. The same scale is used on all y axes for an accurate visual comparison of the convergence times. 10 individual runs have been calculated for both the initial ordered and initial random system. The grey graphs are the cumulative average data from each run, and the black graphs are the averages of all runs. Even though the energy of the system converges much faster than the absolute value of the magnetic moment which never reaches the same convergence as the energy, the system is approximately convergent at $5 \cdot 10^3$ Monte Carlo cycles.

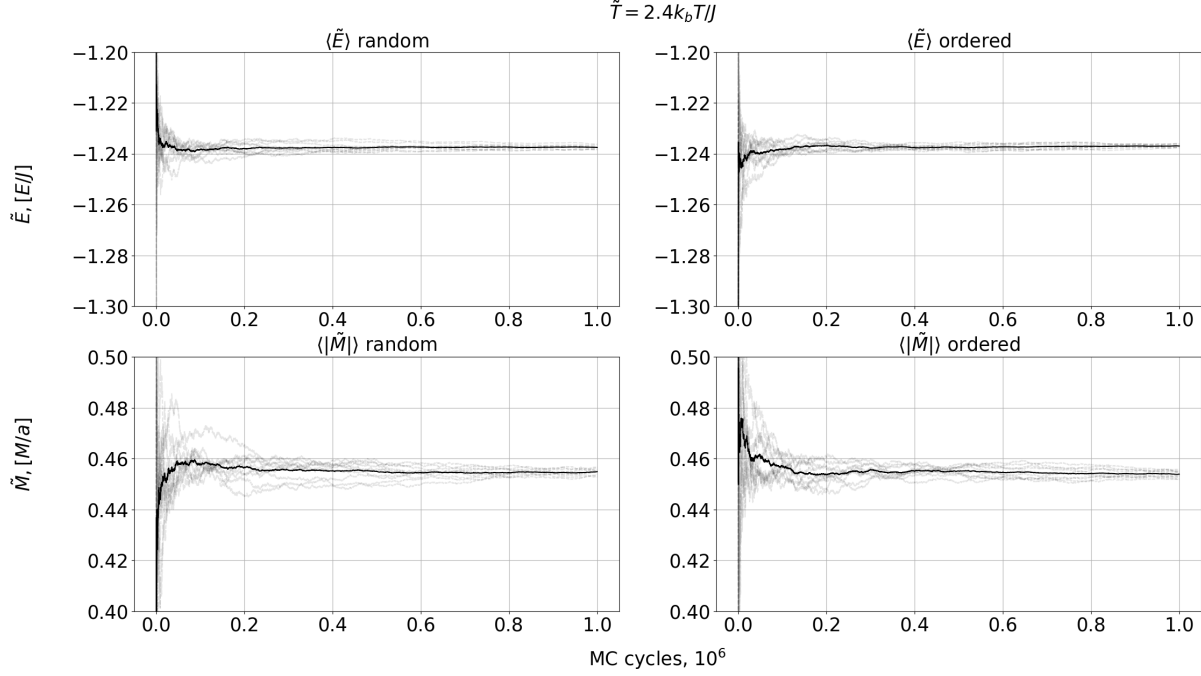


FIG. 2.— $\langle \tilde{E} \rangle$ and $\langle |\tilde{M}| \rangle$ as a function of Monte Carlo cycles at $\tilde{T} = 2.4k_B T/J$ for ordered and random initial states. The y values are scaled with $1/(\text{total spins})$, and the plotted y intervals are of 0.1 function values. The same scale is used on all y axes for an accurate visual comparison of the convergence times. 10 individual runs have been calculated for both the initial ordered and initial random system. The grey graphs are the cumulative average data from each run, and the black graphs are the averages of all runs. The energy and the absolute value of the magnetic moment seems to converge at a similar pace at this scale, with the absolute value of the magnetic moment for the ordered initial state a bit slower than the rest. The system has converged at $4 \cdot 10^5$ Monte Carlo cycles.

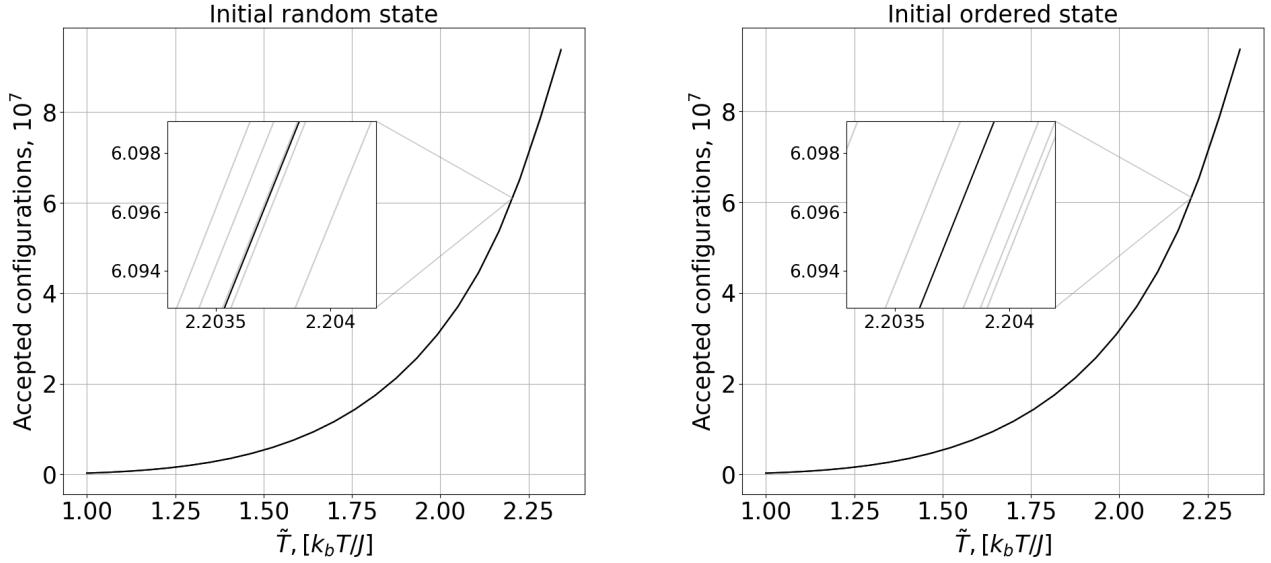


FIG. 3.— The number of accepted configurations as a function of temperature. Five individual runs are displayed as grey graphs and the average of the grey graphs are displayed as the black graphs. A zooming of a selected area is shown to visualize the minuscule differences. 10^6 Monte Carlo cycles were used for all temperature calculations. The difference in the number of accepted configurations is more or less identical for any starting configuration.

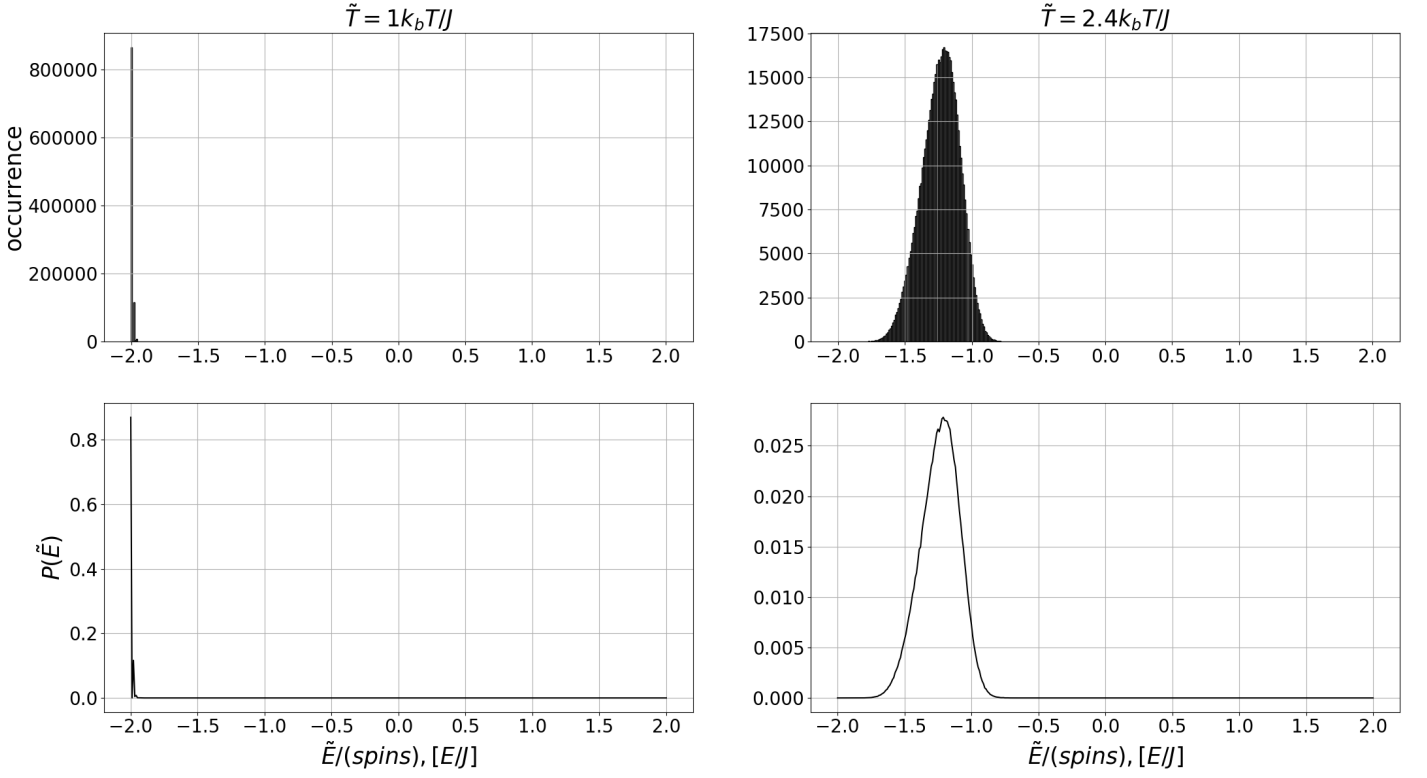


FIG. 4.— Histogram and probability distribution of the total energy, \tilde{E} , of the spin lattice. The energy values are scaled by $\tilde{E}/(\text{number of spins})$ where the number of spins is 20×20 . The left figures represent $\tilde{T} = 1k_B T/J$ and the right figures $\tilde{T} = 2.4k_B T/J$. 10^6 Monte Carlo cycles were used for both temperatures. All data before convergence have been discarded. For $\tilde{T} = 1k_B T/J$ we can see a distribution around $\tilde{E}/(20 \times 20) \approx -2.0E/J$ and for $\tilde{T} = 2.4k_B T/J$ a distribution around $\tilde{E}/(20 \times 20) \approx -1.24E/J$.

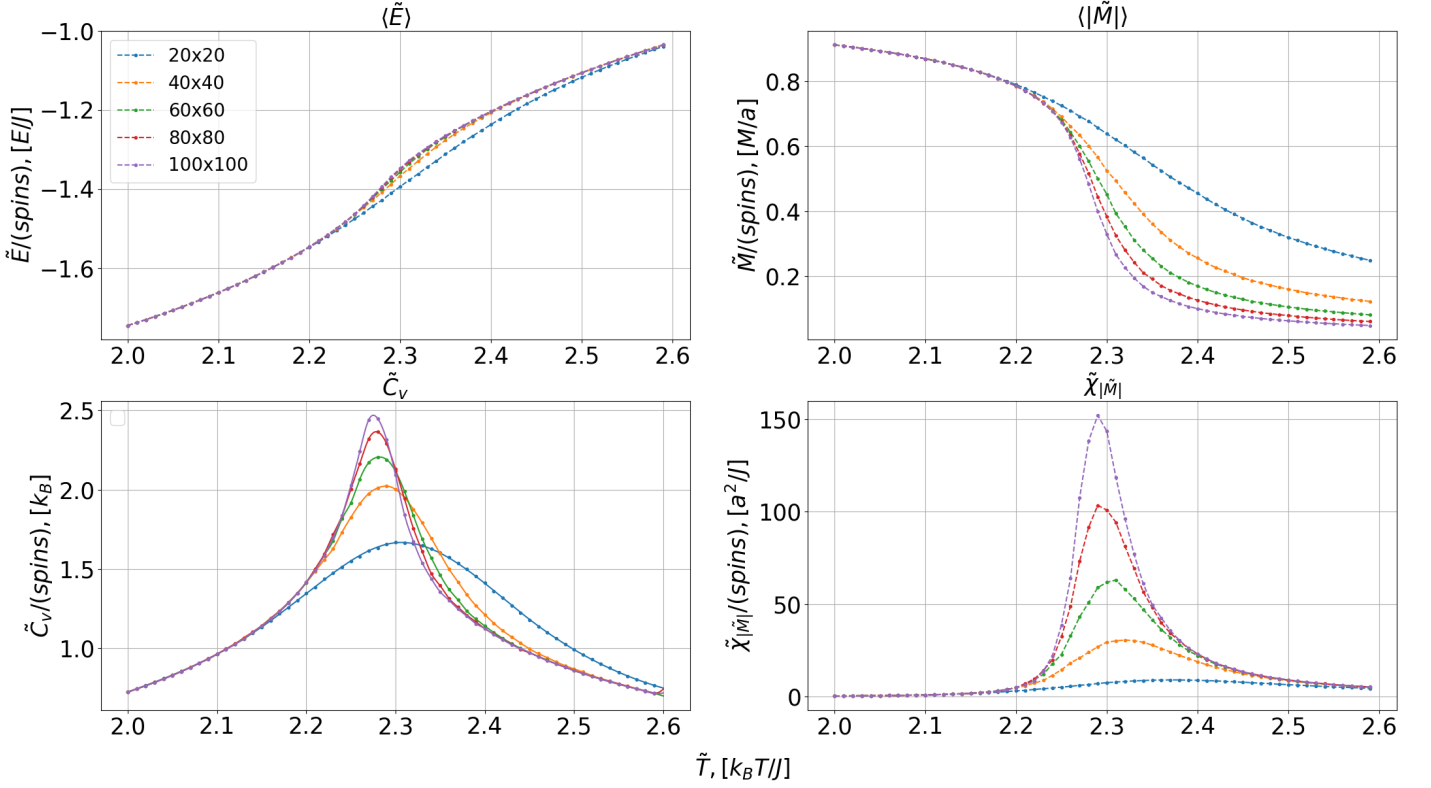


FIG. 5.— $\langle \tilde{E} \rangle$, $\langle |\tilde{M}| \rangle$, \tilde{C}_V , $\tilde{\chi}_{|\tilde{M}|}$ are plotted as a function of temperature for lattices with 20×20 , 40×40 , 60×60 , 80×80 , and 100×100 spins. All y axes are scaled with $1/(\text{number of spins})$. The heat capacity \tilde{C}_V in the bottom left has the calculated data points plotted as dots and interpolations of these points plotted as solid lines of the corresponding color. The interpolation is performed with `scipy.interpolate.UnivariateSpline`. All other plots have only the data points plotted as dots and straight lines connecting each dot.